THEORETICAL AND APPLIED MECHANICS
vol. 26, pp. 33-57, 2001

Impulsive ascension of spherical deforming gas bubbles in a viscous liquid at large Reynolds numbers

Radomir Ašković

Submitted 5 October, 1999

Abstract

An analysis is made for a deforming gas bubble impulsively started to rise with a constant velocity in a quiescent liquid of infinite extent. The disturbed layer is sufficiently large and thus makes possible an important simplification of the governing equations of motion. Simultaneous solution of the unsteady boundary-layer equations for the both outside and inside flows of the bubble are obtained by considering that tangential velocity components and shear stresses on both sides of the interface are equal, while the normal velocity components are given by the velocity of growing of the bubble. Satisfactory results are obtained for spherical deforming air bubbles in water. The theoretical results are applicable to any uniformly deforming fluid sphere started impulsively in a substantially immiscible, viscous liquid provided that the internal circulation is complete, the flow separation is negligible and the Reynolds number is sufficiently large.

1 Introduction

It has been known that a bubble is nearly spherical even when the Reynolds number becomes large, provided that the Weber number

$(2R\rho U_\infty^2/\sigma)$ remains small [1]. Rosenberg [2] performed extensive experiments on the terminal velocity and shape of air bubbles in water. He found that the bubbles were spherical with Reynolds numbers ranging up to about 400. Haberman and Morton [3] presented a table giving the approximate ranges of Reynolds numbers for which air bubbles remain spherical in eight different liquids. Garner and Hammerton [4] reported the existence of regular circulatory currents in gas bubbles rising through liquids using freshly formed ammonium chloride fog. For gas bubbles of diameter greater than 0,03 cm in water, toroidal circulation sets in which increases in vigor with increasing bubble diameter.

Hill [5] analyzed the circulatory motion of an inviscid fluid inside a non deforming sphere due to external irrotational flow. Hill's stream function for such vortex motion is of the form:

$$\Psi_i = -\frac{3}{4}U_\infty \left(1 - \frac{r^2}{R^2}\right) r^2 \sin^2\theta,\ r \leqslant R,$$

where U_∞ is the outside, uniform fluid velocity at infinity, r is the magnitude of the position vector $\vec{r}$ with origin at the bubble center and θ is the angle between $\vec{r}$ and the upstream axis of symmetry. If U_i and V_i denote, respectively, the tangential and radial velocity components, then,

$$\begin{aligned} U_i/U_\infty &= -\frac{3}{2}\left(1 - 2r^2/R^2\right)\sin\theta,\ r \leqslant R, \\ V_i/U_\infty &= \frac{3}{2}\left(1 - r^2/R^2\right)\cos\theta,\ \ r \leqslant R. \end{aligned} \tag{1}$$

The stream function for the external potential flow is well known and is given by

$$\Psi_e = \frac{1}{2}U_\infty \left(1 - R^3/r^3\right) r^2 \sin^2\theta,\ r \geqslant R.$$

The corresponding tangential and radial velocity components are

$$\begin{aligned} U_e/U_\infty &= \left(1 + \frac{1}{2}R^3/r^3\right)\sin\theta,\ r \geqslant R, \\ V_e/U_\infty &= -\left(1 - R^3/r^3\right)\cos\theta,\ r \geqslant R. \end{aligned} \tag{2}$$

Figure 1 shows graphically the tangential velocity distribution both inside and outside of the non deforming fluid sphere at $\theta = \frac{1}{2}\pi$.

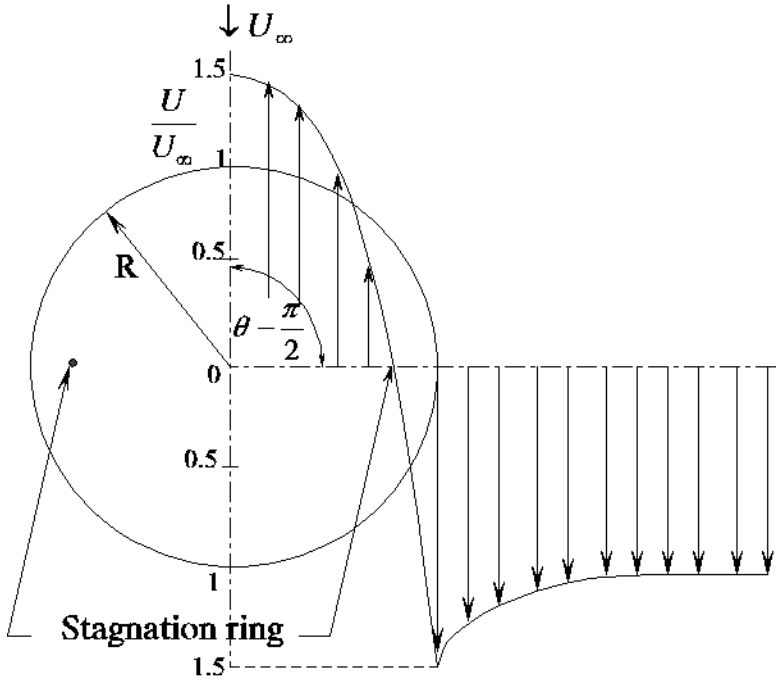

Fig.1. Tangential velocity distribution in the equatorial plane of a fluid sphere

The vorticity distribution is given by

$$\omega = \begin{cases} \dfrac{15}{2} U_\infty \dfrac{r}{R^2} \sin\theta, & r < R, \\ 0, & r > R, \end{cases} \tag{3}$$

which exhibits a discontinuity at the bubble surface except at $\theta = 0$ or π. The sudden jump in vorticity at the fluid interface cannot be physically realized.. It is the consequence of the ideal fluid assumption.

It is to be noticed here that all these considerations are also valid in the case of a uniformly growing bubble ($R = R_0 + A\,t$), started impulsively to rise in a liquid. So, it can be obtained by the perturbation

method that the vorticity distribution will be given by

$$\omega = \begin{cases} \dfrac{15}{2}\dfrac{U_\infty}{R_0}\left(1 - \dfrac{A}{R_0}\,t + \dfrac{1}{5}\dfrac{y}{R_0} - \dfrac{12}{5}\dfrac{y}{R_0}\dfrac{A}{R_0}\,t\right)\sin\theta, & r < R, \\ 6U_\infty\left(-\dfrac{y}{R_0} + \dfrac{y}{R_0}\dfrac{A}{R_0}\,t\right)\sin\theta, & r > R, \end{cases} \tag{4}$$

which confirms the relation (3) in the limiting case $A = 0$ taking into account $\frac{y}{R_0} \ll 1$.

1.1 Boundary layer adjacent to fluid interface

Levich [6] was credited for his first suggesting the concept of a boundary layer over a non deforming fluid interface for analyzing the velocity field associated with bubble motion. Unfortunately, his formulation was in error and his solution incorrect. That is why we are going to use the approach of Chao [7], who corrected this error and proposed a convenient formulation of the corresponding steady problem.

1.2 Mathematical formulation of the unsteady problem

Let us consider the unsteady flow past a fluid sphere whose radius (of initial value R_0) grows uniformly with a constant factor of deformability A:

$$R = R_0 + A\,t, \tag{5}$$

started impulsively at the same time into rectilinear motion, with a constant velocity U_∞, in a viscous, unbounded liquid, initially at rest.

The continuity equation and the Navier-Stokes equation of motion for constant density ρ and viscosity μ are:

a) for outer flow:
Continuity:

$$\nabla \cdot \vec{v}_e = 0 \tag{6}$$

Navier-Stokes equation:

$$\frac{\partial \vec{v}_e}{\partial t} + \vec{v}_e \cdot \nabla \vec{v}_e = -\frac{1}{\rho_e} p_e + \nu_e \Delta \vec{v}_e, \tag{7}$$

where ν_e is the kinematic viscosity, μ_e/ρ_e. The body force due to gravity does not explicitly appear in equation (7) since it may be conveniently incorporated in the pressure term.

It should be noticed here that first Sears [8] in 1949 and then Telionis [9] in 1974 showed that if the motion is started impulsively from rest, the generated field is irrotational and, similarly, even if an impulsive pressure produces a change on an established viscous flow, then this change is also irrotational. In accordance with this idea, we will suppose the solution for the outer flow as follows:

$$\vec{v}_e = \vec{V}_e + \vec{v}'_e, \text{ with } |\vec{v}'_e| \ll \left|\vec{V}_e\right| \tag{8}$$

and

$$p_e = P_e + p', \tag{9}$$

where $\vec{V}_e$ is the velocity field given by the potential solution. Its two components are given by equation (2) including (5). P_e is the pressure field satisfied by equation (11) below. It is identical to that of the irrotational field. In the foregoing expressions, the perturbed quantities are designated by primes. Intuitively, one may assert that considerations of p'_e will be of no consequence since the disturbed layers are thin. This is the usual conclusion one arrives at in ordinary boundary-layer analysis. That such is indeed the case for boundary layers adjacent to the fluid interface was demonstrated in the steady case by Chao [7].

When Eqs.(8) and (9) are introduced into Eqs.(6) and (7), and by virtue of the Sears-Telionis' theorem:

$$\nabla \cdot \vec{V}_e = 0 \tag{10}$$

$$\frac{\partial \vec{V}_e}{\partial t} + \vec{V}_e \cdot \nabla \vec{V}_e = -\frac{1}{\rho_e} \nabla P_e + \nu_e \Delta \vec{V}_e, \tag{11}$$

one obtains for early times of flow development around a uniformly deforming spherical bubble:

$$\nabla \cdot \vec{v}'_e = 0 \tag{12}$$

$$\frac{\partial \vec{v}'_e}{\partial t} + \vec{v}'_e \cdot \nabla \vec{V}_e + \vec{V}_e \cdot \nabla \vec{v}'_e = -\frac{1}{\rho_e} \nabla p'_e + \nu_e \Delta \vec{v}'_e, \tag{13}$$

In equation (13), the term $\vec{v}'_e \cdot \nabla \vec{v}'_e$ has been deleted since it is of smaller order.

b) for inner flow:

A list of equations exactly analogous to Eqs.(6) to (13) can be written for the flow inside the sphere by simply replacing to subscript "e" by "i". Here, V_i, as defined by an expression similar to equation (8), is the velocity field given by Hill's inviscid solution. Its components are given by equation (1). The pressure field P_i satisfies:

$$\frac{\partial \vec{V}_i}{\partial t} + \vec{V}_i \cdot \nabla \vec{V}_i = -\frac{1}{\rho_i} \nabla P_i + \nu_i \Delta \vec{V}_i, \tag{14}$$

1.3 Perturbation method of analysis

Following a procedure suggested by Boltze [10] in his study of boundary layers over a body of revolution, we introduce a curvilinear system of coordinates as shown in Fig.2, which can be considered as Hamiltonian in the case of uniformly increasing (or decreasing) radius of a sphere.

We denote by x the *arc* length measured along any meridian from the front stagnation point, and y the coordinate normal to the bubble surface, outward as positive. For thin boundary layers on the interface, Eqs.(12) and (13), respectively, become (with the latter now written in component form):

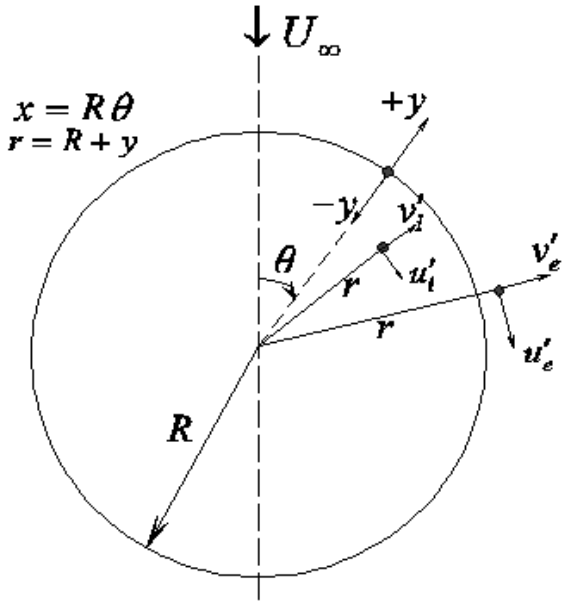

Fig.2. Tangential velocity distribution in the equatorial plane of a fluid sphere

a) for outer flow:

$$\frac{\partial}{\partial x}\left(u'_e \sin\theta\right) + \sin\theta \frac{\partial v'_e}{\partial y} = 0, \tag{15}$$

x direction:

$$\frac{\partial u'_e}{\partial t} + u'_e \frac{\partial U_e}{\partial x} + U_e \frac{\partial u'_e}{\partial x} + v'_e \frac{\partial U_e}{\partial y} + V_e \frac{\partial u'_e}{\partial y} =$$

$$= -\frac{1}{\rho_e}\frac{\partial p'_e}{\partial x} + \nu_e \left(\frac{\partial^2 u'_e}{\partial x^2} + \frac{\partial^2 u'_e}{\partial y^2}\right), \tag{16}$$

in which u'_e is the x (or tangential) component of the perturbed velocity; v'_e is its y (or radial) component. Under the assumption of a thin boundary layer, i.e., $(\delta_e/R) \ll 1$,the following approximations are valid:

$$U_e/U_\infty = \frac{3}{2}\left[\left(1 - \frac{y}{R_0}\right) + \frac{y}{R_0}\frac{A}{R_0}\, t\right]\sin\theta, \;\; y \geqslant 0, \tag{17}$$

$$V_e/U_\infty = -3\left(1 - \frac{A}{R_0}\, t\right)\frac{y}{R_0}\cos\theta,\ y \geqslant 0, \tag{18}$$

$$\left.\begin{aligned} &\text{since: } \frac{y}{R} = \left(1 - \frac{A}{R_0}\, t\right)\frac{y}{R_0}, \\ &\text{and } \frac{R^3}{r^3} = \left(1 + \frac{y}{R}\right)^{-3} = 1 - 3\left(1 - \frac{A}{R_0}\, t\right)\frac{y}{R_0}, \end{aligned}\right\} \quad \begin{aligned} &\text{when } \frac{y}{R_0} \ll 1 \text{ and} \\ &\frac{A}{R_0} t \ll 1. \end{aligned}$$

If we estimate the order of magnitude of each term in the Navier-Stokes equation in the $x-$direction (16), we will obtain, in the case of a gas bubble impulsively started, that $\partial p'_e/\partial x = 0$. It must be pointed out here that, since we consider $x \sim 0(1)$, the analysis cannot be expected to hold at the front stagnation. Substituting the approximate relationships given by Eqs.(17) and (18) into the simplified form of equation (16), gives,

$$\frac{\partial u'_e}{\partial t} + \frac{3}{2}\frac{U_\infty}{R_0}\left(1 - \frac{A}{R_0}\, t\right) \times$$

$$\times \left(u'_e \cos\theta + \frac{\partial u'_e}{\partial \theta}\sin\theta - 2y\cos\theta\frac{\partial u'_e}{\partial y}\right) = \nu_e \frac{\partial^2 u'_e}{\partial y^2}. \tag{19}$$

It is to be noticed that this estimation of the order of magnitude of the terms in the Navier-Stokes equation in the $y-$direction gives that the pressure variation in the $y-$direction is negligeable within the boundary layer ($\partial p'_e/\partial y = 0$). This means that this equation is thus exhausted and needs no further consideration.

b) for inner flow:

For the inner flow, expressions corresponding to Eqs.(17) and (18) are:

$$U_i/U_\infty = \frac{3}{2}\left(1 + 4\frac{y}{R_0} - 4\frac{y}{R_0}\frac{A}{R_0}\, t\right)\sin\theta,\ y \leqslant 0, \tag{20}$$

$$V_i/U_\infty = -3\left(1 - \frac{A}{R_0}\, t\right)\frac{y}{R_0}\cos\theta,\ y \leqslant 0, \tag{21}$$

since

$$\frac{r^2}{R^2} = \left(1 + \frac{y}{R}\right)^2 = 1 + 2\left(1 - \frac{A}{R_0}\, t\right)\frac{y}{R_0}, \text{ when } \frac{y}{R_0} \ll 1 \text{ and } \frac{A}{R_0}\, t \ll 1.$$

By going through a series of arguments analogous to that given for outer flow, one arrives at a simplified equation of motion for u_i'. Here we are going to summarize the results:

Continuity equation:

$$\frac{\partial}{\partial x}\left(u_i' \sin\theta\right) + \sin\theta \frac{\partial v_i'}{\partial y} = 0. \tag{22}$$

Simplified equation of motion for u_i':

$$\frac{\partial u_i'}{\partial t} + \frac{3}{2}\frac{U_\infty}{R_0}\left(1 - \frac{A}{R_0}\, t\right)\left(u_i' \cos\theta + \frac{\partial u_i'}{\partial \theta}\sin\theta - 2y\cos\theta \frac{\partial u_i'}{\partial y}\right) = \nu_i \frac{\partial^2 u_i'}{\partial y^2} \tag{23}$$

Evidently, that these equations (22) and (23) for inner flow are exactly analogous to those (15) and (19) for outer flow.

1.4 Interface conditions

Interface conditions ($y = 0$) are :

$$u_e' = u_i', \tag{24}$$

$$\mu_e \frac{\partial u_e'}{\partial y} - \mu_i \frac{\partial u_i'}{\partial y} = \frac{3}{2}\frac{U_\infty}{R_0}\left(\mu_e + 4\mu_i\right)\left(1 - \frac{A}{R_0}\, t\right)\sin\theta. \tag{25}$$

The first condition is obtained from the "no-slip" condition at the interface, namely,

$$\left(u_e\right)_{y=0} = \left(u_i\right)_{y=0}.$$

Since $\left(U_e\right)_{y=0} = \left(U_i\right)_{y=0}$, equation (24) follows immediately. The second emerges from the requirement of continuity of shear stress, i.e.,

$$\mu_e \left(\frac{\partial u_e}{\partial y}\right)_{y=0} = \mu_i \left(\frac{\partial u_i}{\partial y}\right)_{y=0}.$$

Since

$$u'_e = u_e - U_e, \qquad u'_i = u_i - U_i$$

and

$$\left(\frac{\partial U_e}{\partial y}\right)_{y=0} = -\frac{3}{2}\frac{U_\infty}{R_0}\left(1 - \frac{A}{R_0}t\right)\sin\theta,$$

$$\left(\frac{\partial U_i}{\partial y}\right)_{y=0} = 6\frac{U_\infty}{R_0}\left(1 - \frac{A}{R_0}t\right)\sin\theta,$$

one arrives at equation (25).

In the case of a deforming gas bubble, there is also the interface condition in radial direction:

$$(v'_e)_{y=0} = (v'_i)_{y=0} = \frac{dR}{dt} = A. \tag{26}$$

Conditions at the edge of the disturbed layer:

$$\begin{gathered}(u'_e)_{y=\delta_e} = 0, \text{ for outer flow,} \\ \text{and } (u'_i)_{y=-\delta_i} = 0, \text{ for inner flow,}\end{gathered} \tag{27}$$

where δ_e and δ_i designate, respectively, the thickness of the boundary layer in the outer and in the inner flow.

At this point, one may remark that the solution for the x components of the perturbed velocities, u'_e and u'_i, can be obtained independently of the y components. The mathematical simplification achieved is thus significant. When they are evaluated, the y components of the perturbed velocities can be obtained from the continuity equations.

2 Approximate method of resolution

It has been known since the 1930's that impulsively generated flows around a solid body are initially inviscid. We will consider the same flow development around a radially uniformly deforming sphere, started

impulsively in a viscous liquid initially at rest. Or, after an infinitively small time, the both sides of the interface are covered with vortex sheets which are confined to regions infinitely close to the interface.

Behind this initial period, the most important characteristic of the flow is the concentrated vorticity that needs to be diffused into the flows described by the equations (19) and (23). The diffusion terms will then outweigh all other terms in these equations and will balance the unsteady terms $\partial u'_e/\partial t$ and $\partial u'_i/\partial t$.

So, the integration of the equations (19) and (23) can be carried out by a process of successive approximations:

$$u'_e = \sum_{n=1}^{N} u'_{en}, \qquad u'_i = \sum_{n=1}^{N} u'_{in}, \tag{28}$$

the method being based on the following physical reasoning: in the first instants, after the motion had started from rest, the boundary layers on both sides of the interface are very thin and the viscous diffusion terms. In Eqs.(19) and (23) are very large, comparing to the convective terms. In the frame of the first approximation, these diffusion terms are balanced by the non steady accelerations $\partial u'_e/\partial t$ and $\partial u'_i/\partial t$. The equations for the second and third approximations are then obtained from (19) and (23) in which the convective terms are calculated by using the preceding approximations u'_{e1} and u'_{i1} already known. Hence we have a succession of linear differential equations completed by the continuity equations for each approximation as follows:

a) for outer flow:

$$\frac{\partial u'_{e1}}{\partial t} - \nu_e \frac{\partial^2 u'_{e1}}{\partial y^2} = 0, \tag{29}$$

$$\frac{\partial}{\partial x}\left(u'_{e1}\sin\theta\right) + \sin\theta \frac{\partial v'_{e1}}{\partial y} = 0; \tag{30}$$

$$\frac{\partial u'_{e2}}{\partial t} - \nu_e \frac{\partial^2 u'_{e2}}{\partial y^2} = -\frac{3}{2}\frac{U_\infty}{R_0}\left(1 - \frac{A}{R_0}t\right)\left(u'_{e1}\cos\theta +\right.$$

$$+\frac{\partial u'_{e1}}{\partial \theta}\sin\theta - 2y\cos\theta\frac{\partial u'_{e1}}{\partial y}), \tag{31}$$

$$\frac{\partial}{\partial x}\left(u'_{e2}\sin\theta\right) + \sin\theta\frac{\partial v'_{e2}}{\partial y} = 0 \tag{32}$$

$$\frac{\partial u'_{e3}}{\partial t} - \nu_e\frac{\partial^2 u'_{e3}}{\partial y^2} = -\frac{3}{2}\frac{U_\infty}{R_0}\left(1 - \frac{A}{R_0}t\right)(u'_{e2}\cos\theta +$$

$$+\frac{\partial u'_{e2}}{\partial \theta}\sin\theta - 2y\cos\theta\frac{\partial u'_{e2}}{\partial y}), \tag{33}$$

$$\frac{\partial}{\partial x}\left(u'_{e3}\sin\theta\right) + \sin\theta\frac{\partial v'_{e3}}{\partial y} = 0 \tag{34}$$

– –

a) for inner flow:

$$\frac{\partial u'_{i1}}{\partial t} - \nu_i\frac{\partial^2 u'_{i1}}{\partial y^2} = 0, \tag{35}$$

$$\frac{\partial}{\partial x}\left(u'_{i1}\sin\theta\right) + \sin\theta\frac{\partial v'_{i1}}{\partial y} = 0; \tag{36}$$

$$\frac{\partial u'_{i2}}{\partial t} - \nu_i\frac{\partial^2 u'_{i2}}{\partial y^2} = -\frac{3}{2}\frac{U_\infty}{R_0}\left(1 - \frac{A}{R_0}t\right)(u'_{i1}\cos\theta +$$

$$+\frac{\partial u'_{i1}}{\partial \theta}\sin\theta - 2y\cos\theta\frac{\partial u'_{i1}}{\partial y}), \tag{37}$$

$$\frac{\partial}{\partial x}\left(u'_{i2}\sin\theta\right) + \sin\theta\frac{\partial v'_{i2}}{\partial y} = 0; \tag{38}$$

$$\frac{\partial u'_{i3}}{\partial t} - \nu_i \frac{\partial^2 u'_{i3}}{\partial y^2} = -\frac{3}{2}\frac{U_\infty}{R_0}\left(1 - \frac{A}{R_0}t\right)(u'_{i2}\cos\theta +$$

$$+\frac{\partial u'_{i2}}{\partial \theta}\sin\theta - 2y\cos\theta\frac{\partial u'_{i2}}{\partial y}), \tag{39}$$

$$\frac{\partial}{\partial x}(u'_{i3}\sin\theta) + \sin\theta\frac{\partial v'_{i3}}{\partial y} = 0; \tag{40}$$

– –

Higher-order approximations $u'_{e4}, u'_{i4}, \ldots$ can be obtained in a similar way. However, the complexity of the method of successive approximations increases rapidly as higher approximations are considered.

Of course, the solutions of all these approximations have to be found satisfying the interface and boundary conditions (24) to (27).

2.1 Determination of the tangential velocity components of both external and internal flows

The equations (29) and (35) of the first approximations are identical with that for one-dimensional heat conduction. By introducing the new dimensionless variables η_e and η_i, we found the solutions satisfying the interface and boundary conditions (24) to (27), in the form:

$$u'_{e1} = U_\infty K_1 t^{1/2}\left(e^{-\eta_e^2} - \sqrt{\pi}\eta_e \operatorname{erf} c\ \eta_e\right)\sin\theta, \tag{41}$$

$$u'_{i1} = U_\infty K_1 t^{1/2}\left(e^{-\eta_i^2} - \sqrt{\pi}\eta_i \operatorname{erf} c\ \eta_i\right)\sin\theta, \tag{42}$$

where

$$\eta_e = \frac{y}{2\sqrt{\nu_e\ t}} \tag{43}$$

$$\eta_i = \frac{y}{2\sqrt{\nu_i\, t}} \tag{44}$$

$$K_1 = \frac{3}{\sqrt{\pi}} \frac{\mu_e + 4\mu_i}{\left(\frac{\mu_i}{\sqrt{\nu_i}} - \frac{\mu_e}{\sqrt{\nu_e}}\right)} \frac{1}{R_0}. \tag{45}$$

Inserting then (41) into (31), it results:

$$\frac{\partial u'_{e2}}{\partial t} - \nu_e \frac{\partial^2 u'_{e2}}{\partial y^2} = \left(-t^{1/2} + \frac{A}{R_0} t^{3/2}\right) 3 \frac{U_\infty^2}{R_0} K_1 e^{-\eta_e^2} \sin\theta \cos\theta.$$

If we assume the solution as follows:

$$u'_{e2} = U_\infty K_1 \left[t^{3/2} \left(3 \frac{U_\infty}{R_0}\right) F'_{e2a}(\eta_e) + \right.$$

$$\left. + \, t^{5/2} \left(3 \frac{U_\infty}{R_0} \frac{A}{R_0}\right) F'_{e2b}(\eta_e) \right] \sin\theta \cos\theta, \tag{46}$$

we obtain from the preceding equation the following two differential equations:

$$F'''_{e2a} + 2\eta_e F''_{e2a} - 6F'_{e2a} = 4e^{-\eta_e^2},$$

$$F'''_{e2b} + 2\eta_e F''_{e2b} - 10F'_{e2b} = -4e^{-\eta_e^2},$$

which general solutions are:

$$F'_{e2a}(\eta_e) = C_{e2a} g_{3/2}(\eta_e) - \frac{1}{2} e^{-\eta_e^2},$$

$$F'_{e2b}(\eta_e) = C_{e2b} g_{5/2}(\eta_e) + \frac{1}{3} e^{-\eta_e^2},$$

where:

$$g_\alpha(\eta_e) = \frac{2}{\sqrt{\pi}\Gamma(2\alpha+1)} \int_{\eta_e}^{\infty} (\gamma - \eta_e)^{2\alpha} e^{-\gamma^2} d\gamma.$$

Taking into account the interface and boundary conditions as well as the manner in which the first approximations (41) and (42) are found, the integration constants will be determined by using the following conditions:

$$F_{e2a}^{''}(0) = 0 \text{ and } F_{e2b}^{''}(0) = 0,$$

hence

$$C_{e2a} = 0 \text{ and } C_{e2b} = 0.$$

So, we obtain:

$$F_{e2a}^{'}(\eta_e) = -\frac{1}{2}e^{-\eta_e^2}, \tag{47}$$

$$F_{e2b}^{'}(\eta_e) = \frac{1}{3}e^{-\eta_e^2}. \tag{48}$$

Proceeding analogously, we obtain the solution of the equation (37) for the second approximation of inner flow in the form:

$$u_{i2}' = U_\infty K_1 \left[t^{3/2} \left(3\frac{U_\infty}{R_0} \right) F_{i2a}'(\eta_i) + t^{5/2} \left(3\frac{U_\infty}{R_0}\frac{A}{R_0} \right) F_{i2b}'(\eta_i) \right] \sin\theta\cos\theta, \tag{49}$$

with

$$F_{i2a}^{'}(\eta_i) = -\frac{1}{2}e^{-\eta_i^2}, \tag{50}$$

$$F_{i2b}^{'}(\eta_i) = \frac{1}{3}e^{-\eta_i^2}. \tag{51}$$

Finally, inserting (46) into (33) and seeking the solution as follows:

$$u_{e3}' = t^{5/2} \left(\frac{9}{2}\frac{U_\infty^3}{R_0^2}K_1 \right) \left[\sin\theta \; F_{e3a}'(\eta_e) + \sin^3\theta \; F_{e3b}'(\eta_e) \right] +$$

$$+ t^{7/2} \left(\frac{9}{2}\frac{U_\infty^3}{R_0^2}\frac{A}{R_0}K_1 \right) \left[\sin\theta \; F_{e3c}'(\eta_e) + \sin^3\theta \; F_{e3d}'(\eta_e) \right] +$$

$$+t^{9/2}\left(\frac{9}{2}\frac{U_\infty^3}{R_0^2}\frac{A^2}{R_0^2}K_1\right)\left[\sin\theta\ F'_{e3e}(\eta_e)+\sin^3\theta\ F'_{e3f}(\eta_e)\right], \tag{52}$$

we obtain from equation (33) the following ordinary differential equations:

$$\left.\begin{aligned}
&F'''_{e3a}+2\eta_e F''_{e3a}-10F'_{e3a}=8\left(F'_{e2a}-\eta_e F''_{e2a}\right),\\
&F'''_{e3b}+2\eta_e F''_{e3b}-10F'_{e3b}=4\left(-3F'_{e2a}+2\eta_e F''_{e2a}\right),\\
&F'''_{e3c}+2\eta_e F''_{e3c}-14F'_{e3c}=8\left(-F'_{e2a}+F'_{e2b}+\eta_e F''_{e2a}-\eta_e F''_{e2b}\right),\\
&F'''_{e3d}+2\eta_e F''_{e3d}-14F'_{e3d}=4\left(3F'_{e2a}-3F'_{e2b}-2\eta_e F''_{e2a}+2\eta_e F''_{e2b}\right),\\
&F'''_{e3e}+2\eta_e F''_{e3e}-18F'_{e3e}=8\left(-F'_{e2b}+\eta_e F''_{e2b}\right),\\
&F'''_{e3f}+2\eta_e F''_{e3f}-18F'_{e3f}=4\left(3F'_{e2b}-2\eta_e F''_{e2b}\right),
\end{aligned}\right\} \tag{53}$$

which solutions, satisfying the interface and boundary conditions:

$$F''_{e3a}(0)=F''_{e3b}(0)=F''_{e3c}(0)=0,$$

$$F''_{e3d}(0)=F''_{e3e}(0)=F''_{e3f}(0)=0,$$

$$F'_{e3a}(\infty)=F'_{e3b}(\infty)=F'_{e3c}(\infty)=0,$$

$$F'_{e3d}(\infty)=F'_{e3e}(\infty)=F'_{e3f}(\infty)=0,$$

are found in the form:

$$\left.\begin{aligned}
F'_{e3a}(\eta_e) &= \frac{1}{2}\left(\eta_e^2+\frac{5}{6}\right)e^{-\eta_e^2},\\
F'_{e3b}(\eta_e) &= -\frac{1}{2}\left(\eta_e^2+\frac{7}{6}\right)e^{-\eta_e^2},\\
F'_{e3c}(\eta_e) &= -\left(\frac{2}{3}\eta_e^2+\frac{1}{2}\right)e^{-\eta_e^2},\\
F'_{e3d}(\eta_e) &= \left(\frac{2}{3}\eta_e^2+\frac{17}{24}\right)e^{-\eta_e^2},\\
F'_{e3e}(\eta_e) &= \left(\frac{2}{9}\eta_e^2+\frac{7}{45}\right)e^{-\eta_e^2},\\
F'_{e3f}(\eta_e) &= -\frac{2}{9}\left(\eta_e^2+1\right)e^{-\eta_e^2},
\end{aligned}\right\} \tag{54}$$

By going through an analogous procedure, we determined also the third approximation for inner flow:

$$u'_{i3} = t^{5/2}\left(\frac{9}{2}\frac{U^3}{R_0^2}K_1\right)\left[\sin\theta\ F'_{i3a}(\eta_i)+\sin^3\theta\ F'_{i3b}(\eta_i)\right]+$$

$$+t^{7/2}\left(\frac{9}{2}\frac{U^3}{R_0^2}\frac{A}{R_0}K_1\right)\left[\sin\theta\ F'_{i3c}(\eta_i)+\sin^3\theta\ F'_{i3d}(\eta_i)\right]+$$

$$+t^{9/2}\left(\frac{9}{2}\frac{U^3}{R_0^2}\frac{A^2}{R_0^2}K_1\right)\left[\sin\theta\ F'_{i3e}(\eta_i)+\sin^3\theta\ F'_{i3f}(\eta_i)\right], \tag{55}$$

where:

$$\left.\begin{aligned}
F'_{i3a}(\eta_i) &= \frac{1}{2}\left(\eta_i^2+\frac{5}{6}\right)e^{-\eta_i^2},\\
F'_{i3b}(\eta_i) &= -\frac{1}{2}\left(\eta_i^2+\frac{7}{6}\right)e^{-\eta_i^2},\\
F'_{i3c}(\eta_i) &= -\left(\frac{2}{3}\eta_i^2+\frac{1}{2}\right)e^{-\eta_i^2},\\
F'_{i3d}(\eta_i) &= \left(\frac{2}{3}\eta_i^2+\frac{17}{24}\right)e^{-\eta_i^2},\\
F'_{i3e}(\eta_i) &= \left(\frac{2}{9}\eta_i^2+\frac{7}{45}\right)e^{-\eta_i^2},\\
F'_{i3f}(\eta_i) &= -\frac{2}{9}\left(\eta_i^2+1\right)e^{-\eta_i^2}.
\end{aligned}\right\} \tag{56}$$

2.2 Determination of the normal velocity components of both outer and inner flows

According to the relations of transformation of coordinates:

$$\frac{\partial}{\partial x}=\frac{1}{R_0+At}\frac{\partial}{\partial\theta}=\frac{1}{R_0}\left(1-\frac{A}{R_0}t\right)\frac{\partial}{\partial\theta},\qquad dy=2\sqrt{\nu_e t}d\eta_e,$$

the continuity equation for the first approximation of outer flow (30) becomes:

$$\sin\theta\frac{\partial v'_{e1}}{\partial y}+\frac{1}{R_0}\left(1-\frac{A}{R_0}t\right)\frac{\partial}{\partial\theta}\left(u'_{e1}\sin\theta\right)=0.$$

Hence, multiplying by $dy=2\sqrt{\nu_e t}d\eta_e$ and by integration, respecting the interface condition $\left(v'_{e1}\right)_{y=0}=A$, we obtain:

$$\frac{v'_{e1}}{U_\infty}=\frac{A}{U_\infty}-4\frac{\sqrt{\nu_e}}{R_0}K_1\left(1-\frac{A}{R_0}t\right)t\times$$

$$\times \left[\frac{\sqrt{\pi}}{4} + \frac{1}{2}\eta_e e^{-\eta_e^2} - \frac{\sqrt{\pi}}{2}\left(\frac{1}{2} + \eta_e^2\right) \operatorname{erf} c\ \eta_e \right] \cos\theta. \tag{57}$$

Analogously, we found the solution of the equation (36) for the first approximation of inner flow in the radial direction:

$$\frac{v'_{i1}}{U_\infty} = \frac{A}{U} - 4\frac{\sqrt{\nu_i}}{R_0} K_1 \left(1 - \frac{A}{R_0}t\right) t\times$$

$$\times \left[\frac{\sqrt{\pi}}{4} + \frac{1}{2}\eta_i e^{-\eta_i^2} - \frac{\sqrt{\pi}}{2}\left(\frac{1}{2} + \eta_i^2\right) \operatorname{erf} c\ \eta_i \right] \cos\theta. \tag{58}$$

Inserting (46) into (32), then by integration and taking into account of the interfacial condition $(v'_{e2})_{y=0} = 0$,we obtain for outer flow:

$$\frac{v'_{e2}}{U_\infty} = 2\sqrt{\nu_e}\left(1 - \frac{A}{R_0}t\right) K_1 \left[t^2 \left(3\frac{U_\infty}{R_0^2}\right) F_{e2a}(\eta_e) + \right.$$

$$\left. + t^3 \left(3\frac{U_\infty}{R_0^2}\frac{A}{R_0}\right) F_{e2b}(\eta_e) \right] \left(3\sin^2\theta - 2\right), \tag{59}$$

as well as for inner flow:

$$\frac{v'_{i2}}{U_\infty} = 2\sqrt{\nu_i}\left(1 - \frac{A}{R_0}t\right) K_1 \left[t^2 \left(3\frac{U_\infty}{R_0^2}\right) F_{i2a}(\eta_i) + \right.$$

$$\left. + t^3 \left(3\frac{U_\infty}{R_0^2}\frac{A}{R_0}\right) F_{i2b}(\eta_i) \right] \left(3\sin^2\theta - 2\right). \tag{60}$$

It is also possible to determine the third approximations from both outer and inner flows in the radial direction, beginning from the equations (34) and (40), and using the expressions (52) and (55).

3 Computation of velocity profiles

The distribution of two velocity components, tangential and radial, for both outer and inner flows, in function of: deformability factor

$\left(\frac{A}{U_\infty}\right.$ and $\left.\frac{AT}{U_\infty}\right)$, dimensionless time $\left(\frac{U_\infty t}{R_0} = T\right)$ and Reynolds numbers $\left(\frac{2R_0U_\infty}{\nu_e} = R_{ee},\ \frac{2R_0U_\infty}{\nu_i} = R_{ei} = \frac{\nu_e}{\nu_i}R_{ee}\right)$, is computed at the equatorial plane $\left(\theta = \frac{\pi}{2}\right)$, of a uniformly deforming air bubble rising in water, by using all the solutions previously obtained, namely (41), (42), (46), (49), (52), (55), (57), (58), (59), (60), adapted into non dimensional form as follows:

$$\frac{u_e}{U_\infty} = \frac{U_e}{U_\infty} + \frac{u'_e}{U_\infty} = \frac{3}{2}\left[1 - \left(1 - \frac{AT}{U_\infty}\right)\frac{y}{R_0}\right] -$$

$$-2.62\frac{T^{1/2}}{\sqrt{R_{ee}}}\left(e^{-\eta_e^2} - \sqrt{\pi}\eta_e \operatorname{erf} c\ \eta_e\right) +$$

$$+\frac{T^{5/2}}{\sqrt{R_{ee}}}\left[1.965 - 2.45625\left(\frac{AT}{U_\infty}\right) + 0.786\left(\frac{AT}{U_\infty}\right)^2\right]e^{-\eta_e^2} \tag{61}$$

$$\frac{v_e}{U_\infty} = \frac{V_e}{U_\infty} + \frac{v'_e}{U_\infty} =$$

$$= \frac{A}{U_\infty} + 9.851\left[1 - \frac{5}{3}\left(\frac{AT}{U_\infty}\right) + \frac{2}{3}\left(\frac{AT}{U_\infty}\right)^2\right]\frac{T^2}{R_{ee}}\operatorname{erf}\ \eta_e, \tag{62}$$

$$\eta_e = \frac{y}{2\sqrt{\nu_e t}} = \frac{1}{2\sqrt{2}}\left(\frac{R_{ee}}{T}\right)^{1/2}\frac{y}{R_0}; \tag{63}$$

$$\frac{u_i}{U_\infty} = \frac{U_i}{U_\infty} + \frac{u'_i}{U_\infty} = \frac{3}{2}\left[1 + 4\left(1 - \frac{AT}{U_\infty}\right)\frac{y}{R_0}\right] -$$

$$-2.62\sqrt{\frac{\nu_e}{\nu_i}}\frac{T^{1/2}}{\sqrt{R_{ei}}}\left(e^{-\eta_i^2} - \sqrt{\pi}\eta_i \operatorname{erf} c\ \eta_i\right) +$$

$$+\sqrt{\frac{\nu_e}{\nu_i}}\frac{T^{5/2}}{\sqrt{R_{ei}}}\left[1.965-2.45625\left(\frac{AT}{U_\infty}\right)+0.786\left(\frac{AT}{U_\infty}\right)^2\right]e^{-\eta_i^2} \quad (64)$$

$$\frac{v_i}{U_\infty}=\frac{V_i}{U_\infty}+\frac{v_i'}{U_\infty}=$$

$$=\frac{A}{U_\infty}-77.92564\frac{\nu_e}{\nu_i}\frac{T^2}{R_{ei}}\left[1-\frac{5}{3}\left(\frac{AT}{U_\infty}\right)+\frac{2}{3}\left(\frac{AT}{U_\infty}\right)^2\right]\text{erf }\eta_i, \quad (65)$$

$$\eta_i=\frac{y}{2\sqrt{\nu_i t}}=\frac{1}{2\sqrt{2}}\left(\frac{R_{ei}}{T}\right)^{1/2}\frac{y}{R_0}. \quad (66)$$

Figures 3 to 6 illustrate this computation in the case of AIR BUBBLES RISING IN WATER at 20^0C, where:

$$\rho_i/\rho_e=0.0012 \text{ and } \mu_i/\mu_e=0.019.$$

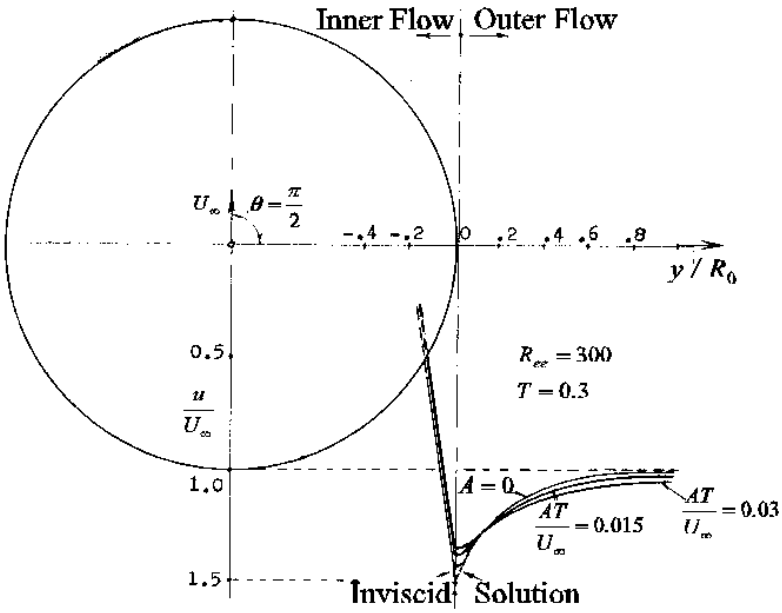

Fig.3. Tangential velocity distribution in the equatorial plane for deforming air bubbles rising in water at different deformability factors

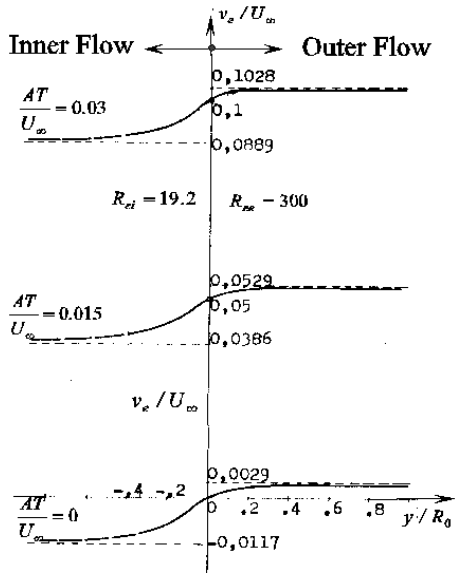

Fig.4. Instantaneous radial velocity distribution in equatorial plane for uniformly growing air bubbles rising in water at different deformability factors

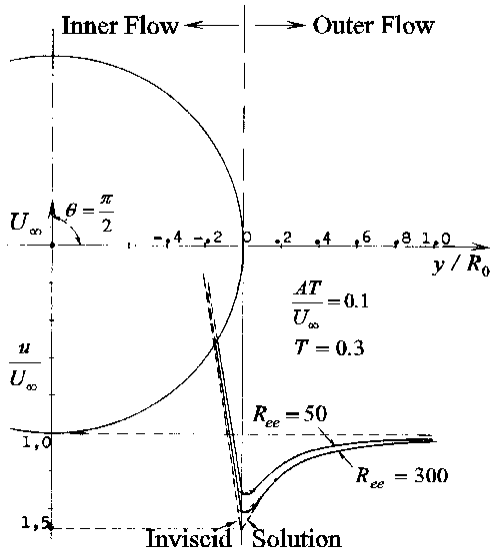

Fig.5. Instantaneous radial velocity distribution in equatorial plane for uniformly growing air bubbles rising in water at different Reynolds numbers

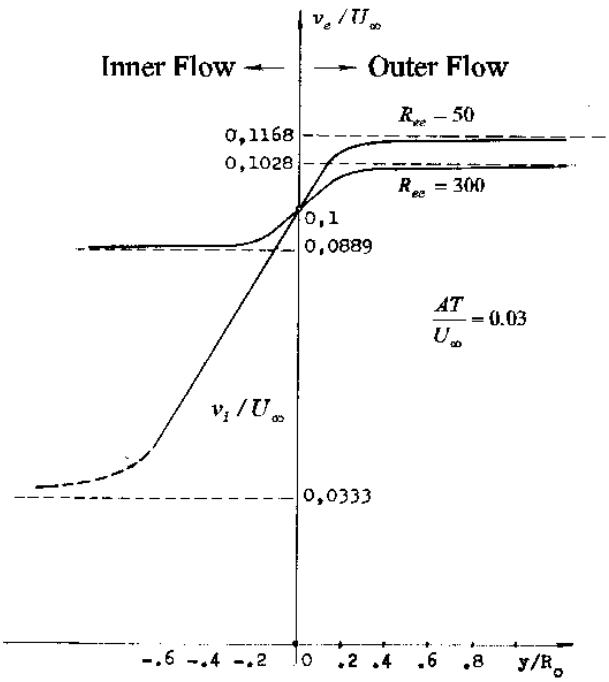

Fig.6. Radial velocity distribution in equatorial plane of the growing air bubbles at $AT/U_\infty = 0.03$ and for two Reynolds numbers

4 Conclusion

Now we are studying the problem of deforming spherical gas bubbles impulsively rising in some organic liquids (such as the methyl alcohol at $30^0 C$ for instance). All the results, either these presented here or those for organic liquids seem to be entirely satisfactory. So as expected, the tangential velocity at the interface decreases when the deformability factor A increases, while the effect is just opposite sufficiently far from the interface (fig.3), because of the pushing forward effect. But the growing bubble causes a big difference especially in radial velocity distribution, comparing to the non deformable case (fig.4), which probably could have significant sequels to the drag force of a spherical deforming bubble. That will be our next subject of study.

Figures 5 and 6 show that the boundary layer becomes evidently thinner as the Reynolds number is increased, for every particular value

of deformability factor and at each instant of time.

Inasmuch as the present analysis is developed under the assumption that the perturbed velocity is small as compared to the velocity given by the inviscid solution, as well as taking into account the applied method of successive approximations, we can expect the solution to hold at early times, and not in the region close to the rear stagnation to hold at early times, and not in the region close to the rear stagnation point. That is why only a portion of the velocity profile inside the bubble is shown since, according to the inviscid solution, the radius of the stagnation ring in the equatorial plane is $\sqrt{2}/2$ of the bubble radius (figure 1). Due to the small-perturbation hypothesis used in the analysis, the both outer and inner velocity fields are considered to be accurate only in the vicinity of the interface.

Finally, all the shapes of velocity profiles for both external and internal flows, given in figures 3 to 6, are compatible to those recently obtained [12] in the case of impulsive ascension of a non deforming spherical gas bubble. Likewise. to confirm our results presented here, we also intend to solve the equations (19) and (23) by direct numerical integration similarly as in [11].

References

[1] D.W.Moore, J.Fluid Mech.6, 113 (1959).

[2] B.Rosenberg, David Taylor Model Basin Rept. 727 (1953).

[3] W.L.Haberman and R.K.Morton, David Taylor Model Basin Rept. 802 (1953); also, Trans.Am.Soc.Civil Engrs. 121 (1956), 227.

[4] F.H.Garner and D.Hammerton, Chem.Eng.Sci. 3 (1954), 1.

[5] L.M.Milne-Thomson, Theoretical Hydrodynamics, 4 th ed., p.554; The MacMilian Company, New York, 1960.

[6] V.G.Levich, Zhur.Eksptl. i Teoret.Fiz. 19 (1949), 18.

[7] B.T.Chao, Physics of Fluids, Vol.5, N1 (1962), 69-79.

[8] W.R.Sears, Introduction to Theoretical Hydrodynamics, Cornell Univ.Press, Ithaca, 1949.

[9] Telionis D.P. and Tsahalis D.T., Acta Astron. 1 (1974), 1487-1505.

[10] E.Boltze, Grenzscichten an Rotationskorpern. Göttingen, 1908.

[11] S.Hanchi & R.Askovic & L.T.Phuoc, Numerical simulation of a flow around an impulsively started radially deforming circular cylinder. Int.J. for Numer.Methods in Fluids 29 (1999), 555-573.

[12] R.Askovic, Impulsive motion of spherical gas bubbles in a viscous liquid at large Reynolds numbers, Submitted.

R.Ašković
Laboratoire de Mécanique et d'Energétique
Université de Valenciennes
Le Mont Houy - B.P. 311
59304 Valenciennes
France

Impulsivno kretanje deformabilnog sfernog gasnog mehura kroz viskoznu tecnost

UDK 532.526; 533.15

U radu se rešava problem impulsivnog kretanja sfernog gasnog mehura uniformno rastućeg poluprečnika kroz viskoznu tečnost pri dovoljno velikim Rejnoldsovim brojevima, primenjujući koncept formiranja spoljašnjeg i unutrašnjeg graničnog sloja u odnosu na opnu (interface) mehura. Dobijena su simultana približna rešenja oba nestacionarna granična sloja, spoljašnjeg i unutrašnjeg, uz zadovoljavanje svih graničnih uslova, posebno na površini opne: uslovi "neklizanja" i kontinuiteta tangencijalnih napona, dok je radijalna brina definisana brinom rasta mehura. Predložena metoda je testirana na primeru kretanja vadušnog mehura u vodi, sa zadovoljavajućim rezultatima.